Two-magnon scattering and viscous Gilbert damping in ultrathin ferromagnets

K. Lenz,* H. Wende, W. Kuch, and K. Baberschke
Institut für Experimentalphysik, Freie Universität Berlin, Arnimallee 14, D-14195 Berlin, Germany

K. Nagy and A. Jánossy
Budapest University of Technology and Economics, Institute of Physics, Solids in Magnetic Fields Research Group of the Hungarian Academy of Sciences, H-1521 Budapest, P.O. Box 91, Hungary

(Received 30 November 2005; published 20 April 2006)

Ferromagnetic resonance experiments of magnetic nanostructures over a large frequency range from 1 to 225 GHz are presented. We find unambiguous evidence for a nonlinear frequency dependence of the linewidth. The viscous Gilbert damping and two-magnon scattering are clearly separated. Both angular and frequency dependent measurements give a transverse scattering rate within the magnetic subsystem of the order of 10^9 s^{-1}, whereas the longitudinal Gilbert relaxation into the thermal bath is one to two orders of magnitude smaller.

DOI: 10.1103/PhysRevB.73.144424 PACS number(s): 76.60.Es, 76.50.+g, 75.40.Gb, 72.25.Rb

I. INTRODUCTION

The investigation of the magnetization dynamics in magnetic nanostructures is among the most fascinating research projects. In magnetic memory devices, for example, a clear understanding of the basic mechanisms is required to analyze the dynamics of a reversal or excitation of the magnetization of ferromagnetic domains on a picosecond time scale. The Landau-Lifshitz equation of motion, extended by the Gilbert-damping term (LLG equation),[1,2]

$$\frac{\partial \vec{M}}{\partial t} = -\gamma(\vec{M} \times \vec{H}_{\text{eff}}) + \frac{G}{\gamma M_s^2}\left[\vec{M} \times \frac{\partial \vec{M}}{\partial t}\right] \qquad (1)$$

is the most popular assumption for the description of the dynamics of the magnetization $\vec{M}$, in ferromagnets. Here, γ is the absolute value of the gyromagnetic ratio and M_s is the saturation magnetization. The first term on the right-hand side of Eq. (1) describes the precession of the magnetization in the effective field $\vec{H}_{\text{eff}}$ that includes the external, demagnetization, and crystalline anisotropy fields. In the absence of damping, this leads to the Larmor precession with a well defined frequency, ω. All real systems have some finite damping, which for small perturbations out of the equilibrium is given by the well-known Gilbert damping, i.e., the second term of Eq. (1), see, e.g., the reviews in Refs. 3 and 4. Two notations are commonly used: (i) G, the Gilbert-damping parameter, given as a relaxation rate in s^{-1}, or (ii) the dimensionless parameter $\alpha = G/\gamma M_s$ in analogy to the viscous damping parameter in mechanical friction. The relaxation rate per second, G, is more instructive, but we tabulate both quantities, α and G, for easier comparison of our experimental results with literature.

Ferromagnetic resonance (FMR) is one of the standard tools to study the magnetic state excited out of the thermodynamic equilibrium.[5,6] At resonance, $\hbar\omega = g\mu_B H_{\text{eff}}$, the microwave excitation induces a uniform motion of the magnetization (i.e., a spin wave mode with a wave vector $\vec{k} \approx 0$). In general, the homogeneous resonance linewidth is given by relaxation processes depicted in Fig. 1. The viscous (velocity-proportional) damping of the magnetization, described by Eq. (1), leads to a direct dissipation of energy into the thermal bath. We denote this *irreversible* process in Fig. 1 by path No. 1.

It is well-known that in addition to the irreversible dissipative path No. 1 a second process is possible in paramagnetic and ferromagnetic resonance, namely, the scattering within the magnetic subsystem. In this case the uniform motion of the magnetization (during precession or reversal of the magnetization) may populate excited states *within* the magnetic system (higher energy magnons, Stoner excitations, etc.). These processes may be reversible and are indicated in Fig. 1 as path No. 2. They are in full analogy to optical spectroscopy. In the long run these excitations will also decay into the thermal bath as indicated by path No. 3. One may raise the question: Is there any experimental evidence for the appearance of this additional path, i.e., scattering within the magnetic subsystem, in magnetic nanostructures? The theoretical background to study this question was known for a long time. One possible model is described by the Bloch-Bloembergen equation[8]

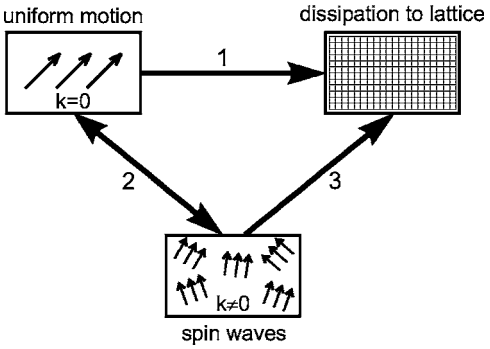

FIG. 1. Paths for degradation of uniform motion: (1) Direct relaxation to the lattice. (2) Decay into nonuniform motions (spin waves), (3) which in turn decay to the lattice (from Ref. 7).

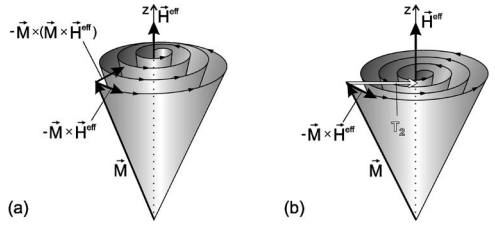

FIG. 2. Relaxation of the precession of $\vec{M}$ according to (a) the LLG equation, i.e., $|\vec{M}|$=const. and (b) the Bloch-Bloembergen equation of motion ($|M_z|$=const.).

$$\frac{\partial \vec{M}}{\partial t} = -\gamma(\vec{M}\times\vec{H}_{\text{eff}}) - \frac{M_x}{T_2}\hat{e}_x - \frac{M_y}{T_2}\hat{e}_y - \frac{M_z - M_s}{T_1}\hat{e}_z, \quad (2)$$

where $\hat{e}_i$ $(i=x,y,z)$ are Cartesian unit vectors. In this case, two different relaxation rates are introduced into the equation of motion:[9] the longitudinal relaxation rate T_1, i.e., the direct path into the thermal bath, and the so-called transverse rate, T_2, by which energy is scattered into the transverse magnetization components M_x and M_y. Figure 2 shows schematically the precession of the magnetization. Figure 2(a) depicts the LLG scenario from Eq. (1). The viscosity damps the Larmor precession, and the magnetization spirals into the z axis pointing to the surface of a sphere, i.e., the length of $\vec{M}$ stays constant but the expectation value of M_z increases. Figure 2(b) shows the Bloch-Bloembergen process for spin-spin relaxation. The projection of $\vec{M}$ onto the z axis stays constant if $T_1 \gg T_2$, since the precessional energy is scattered into the transverse components M_x and M_y.

II. FMR EXPERIMENTS

In the standard FMR technique the microwave frequency is kept constant and the external magnetic field is swept through the resonance. Under this condition, the linewidth derived from Eq. (1) is[10]

$$\Delta H_{\text{G}}(\omega) \approx \frac{2}{\sqrt{3}}\frac{G}{\gamma^2 M}\frac{\omega}{\cos\beta}, \quad (3)$$

i.e., the experimentally determined linewidth, ΔH depends linearly on the microwave frequency ω. β is the angle between $\vec{M}$ and $\vec{H}$. This linewidth can be regarded as the result of relaxation path No. 1 in Fig. 1. Recently Mills and co-workers[11–13] have discussed and calculated the FMR linewidth contribution from two-magnon scattering for magnetic nanostructures as an important mechanism corresponding to path No. 2 in Fig. 1. Unlike the Gilbert damping of Eq. (1), the analytical frequency dependence of this two-magnon process is not linear in ω. It shows a very steep nonlinear slope at low frequencies and a saturation at high frequencies:[11–13]

$$\Delta H_{2\text{M}}(\omega) = \Gamma \sin^{-1}\sqrt{\frac{\sqrt{\omega^2 + (\omega_0/2)^2} - \omega_0/2}{\sqrt{\omega^2 + (\omega_0/2)^2} + \omega_0/2}}, \quad (4)$$

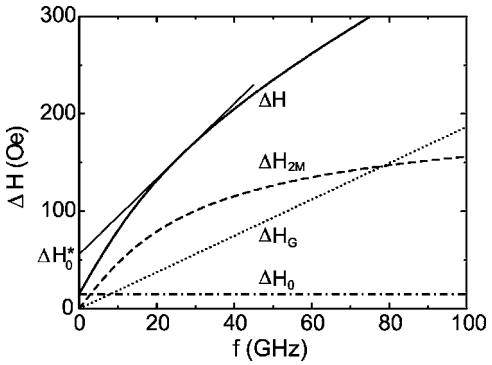

FIG. 3. Schematic diagram of the frequency dependence of the various linewidth contributions.

with $\omega_0 = \gamma 4\pi M_{\text{eff}}$. The effective magnetization $4\pi M_{\text{eff}}$ includes the anisotropy fields. It is therefore obvious that FMR experiments over a large range of frequencies will give an unambiguous answer whether only viscous energy dissipation (longitudinal damping) or also some more complicated processes contribute to the FMR linewidth, i.e., to the damping of the motion of the magnetization. The prefactor Γ in Eq. (4) (Ref. 14) gives the strength of the two-magnon scattering and will be compared to the Gilbert-damping constant G. Figure 3 schematically shows the expected contributions to the linewidth as a function of frequency. If the Gilbert damping, characterized by α or G, described the full magnetization dynamics then one would expect a linear increase of the FMR linewidth with frequency (dotted line in Fig. 3) according to Eqs. (1) and (3). The dashed line shows the linewidth from damping by two-magnon scattering $\Delta H_{2\text{M}}$ as calculated by Arias and Mills [see Eq. (4)]. For experimental reasons one also might have some inhomogeneous residual linewidth ΔH_0 (dashed-dotted line). The sum of the three contributions is indicated by the full line ΔH. Unfortunately, the microwave FMR technique has a technical handicap. Usually only discrete microwave frequencies covering a small range are available, and most often there are only two frequencies at about 9 and 36 GHz. Clearly, a limited set of low frequency experimental data can always be fitted with a linear frequency dependence and a constant inhomogeneous term.[15] If, however additional data are taken at higher frequencies, for example at 70–100 GHz, then a weaker slope will be found together with a different intercept at zero frequency denoted by the apparent residual linewidth ΔH_0^* on the schematic drawing of Fig. 3. Since frequencies up to THz are available in modern spectrometers,[16,17] the way out is to measure the FMR over a very large frequency range. First indications of a nonlinear frequency dependence $\Delta H(\omega)$ have been published by us recently.[18] Here we extend the frequency range and present FMR data from 1 GHz to higher than 200 GHz.

Two multilayer samples $[Fe_4/V_2]_{60}$ and $[Fe_4/V_4]_{45}$ with 60 and 45 repetitions of the Fe/V layers, respectively, grown on MgO(001), were investigated. The subscripts in Fe_4/V_2 and Fe_4/V_4 denote the number of atomic monolayers, ML. Details of sample preparation and characterization are published elsewhere.[19–21] The FMR experiments were carried out using different FMR setups at ambient temperature.[22] In

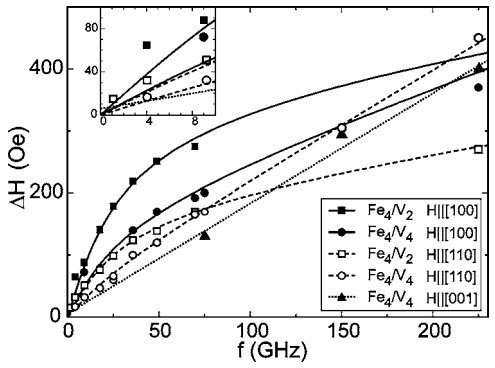

FIG. 4. Resonance linewidths of two Fe/V multilayer samples as a function of microwave frequency. The inset is a magnification of the low frequency regime. Error bars are within symbol size.

addition, we analyze some published FMR results[23] on the nonlinear frequency dependence of the FMR linewidth from the literature.

III. RESULTS AND DISCUSSION

The two key results of our FMR experiments are the following: (i) FMR experiments in a frequency range of more than two orders of magnitude show an unambiguous nonlinear frequency dependence of the linewidth $\Delta H(\omega)$. We will show by reanalyzing published data that this feature is not specific to the present Fe/V multilayers but may be also identified in Pd-capped Fe films deposited on GaAs.[23] (ii) In addition, we present magnetic field-angle dependent measurements of the linewidth for our Fe/V multilayers, which allow us to separate longitudinal and transverse relaxations, i.e., the Gilbert damping from the T_2-Bloch-Bloembergen contribution.

The frequency dependencies of the resonance linewidths for the Fe/V multilayer samples are shown in Fig. 4 for three different directions of the external magnetic field. The solid and dashed curves for the $\vec{H}\|[100]$ and [110] in-plane directions are fits using a sum of Eqs. (3) and (4). For the dotted line for the [001] out-of-plane direction an inhomogeneous contribution ΔH_0 is included. The fit parameters for these fitting curves are listed in Table I. The FMR experiments with the external field applied in the film plane show all a curved nonlinear frequency dependence. In contrast, the dataset with $\vec{H}\|[001]$, i.e., perpendicular to the film plane (dotted line in Fig. 4), shows a linear frequency dependence up to more than 200 GHz. It is in full agreement with the theoretical predictions: Two-magnon scattering is not effective in FMR when $\vec{H}$ is perpendicular to the film plane, but may be very important for various directions of the external field applied in the film plane. It is interesting to note that for obtaining the correct frequency dependence of ΔH very low frequencies (below 9 GHz) (Ref. 18) are as important as very high frequencies (225 GHz). Clearly, the high frequency data of 75, 150, and 225 GHz show us the "saturation effect" of Eq. (4) for the two-magnon scattering, but the very low frequency datapoint at 1 GHz (inset of Fig. 4) tells us clearly that within an experimental error we do not see any "residual linewidth" ΔH_0 or extrapolated ΔH_0^* bigger than 15 Oe. In fact, the linewidth at 1 GHz narrows to 15 Oe. The residual linewidth is consequently very small and the values listed in the last column of Table I, obtained from fitting to the theoretical curves, are zero or a few Oe. Thus inhomogeneous magnetic fields and linewidth broadening are not important for the present experiments; all contributions to the linewidth are the result of various spin relaxation processes.

TABLE I. Linewidth parameters for the Fe/V superlattices measured in field $\vec{H}$ parallel to [100], [110], and [001] directions. The error bars of the numbers given below are of the order of 10%. They depend mainly on the values of M_s, g, and the anisotropy fields.

Sample	Orientation	Γ (Oe)	$\gamma\Gamma$ (10^8 s^{-1})	G (10^8 s^{-1})	α (10^{-3})	ΔH_0 (Oe)
Fe_4/V_2	$\vec{H}\|[100]$	280	51.9	0.20	0.97	0
Fe_4/V_4	$\vec{H}\|[100]$	139	26.1	0.45	2.59	0
Fe_4/V_2	$\vec{H}\|[110]$	150	27.9	0.22	1.06	0
Fe_4/V_4	$\vec{H}\|[110]$	45	8.4	0.77	4.44	0
Fe_4/V_4	$\vec{H}\|[001]$	0	0	0.76	4.38	6

We argue that the Gilbert damping is not an arbitrary and ambiguous fitting parameter but rather it is a velocity proportional viscous damping. Moreover, G is independent of frequency within a small uncertainty for a given sample. We find for the $[Fe_4/V_4]_{45}$ sample a Gilbert parameter of $G = 0.76 \times 10^8$ s^{-1} for both the out-of-plane and [110] in-plane directions.

For the $(Fe_4/V_2)_{60}$ sample the value of G is approximately three times smaller, but also in the range of 10^7 s^{-1}. Let us now compare the prefactor G of Eq. (3) with the prefactor Γ of Eq. (4), i.e., the two-magnon scattering parameter listed in column 3 of Table I. First of all, with the field applied perpendicular to the film plane, the two-magnon scattering is zero. In contrast, for both in-plane orientations and both samples we do not only observe a two-magnon scattering contribution, but it is also larger than the viscous Gilbert-damping.

For easier comparison of Γ with G, we list in column 4 of Table I the product $\gamma \cdot \Gamma$ in 10^8 s^{-1}. We conclude that for both samples the two-magnon scattering is largest along the [100] direction and 2–3 times smaller along the [110] direction. This can be explained in the framework of the model of Arias and Mills.[11,13] There, the two-magnon scattering is mediated by islandlike surface/interface defects of rectangular shape with parallel sides. The shape enters directly into Γ.[11] Thus, the data would be consistent with this model, if the interface defects were mainly oriented along the [100] direction. A comparison between the Fe_4/V_2 and Fe_4/V_4 samples shows that in the former with only 2 ML of V the two-magnon scattering is larger by a factor of 2 than in the sample with 4 ML V. This is plausible within the theory, since the thinner the nonmagnetic V spacer is the more important are terraces and squarelike perturbations.

We apply the same type of analysis and fitting procedure to FMR experiments on a 30 ML Fe film on GaAs(001)

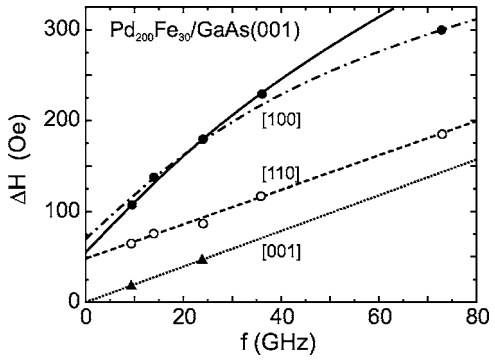

FIG. 5. Frequency dependence of the resonance linewidth of $Pd_{200}Fe_{30}/GaAs(001)$ taken from Ref. 23.

capped with 200 ML Pd published by Woltersdorf and Heinrich in Fig. 5 of Ref. 23 to determine G and Γ. The result is shown in Fig. 5 and Table II. Woltersdorf and Heinrich also discuss their findings within the framework of Gilbert damping and two-magnon scattering. However, in contrast to our analysis, they only provide a guide to the eye for the frequency dependent measurements along the [100] direction and do not analyze the nonlinear frequency dependence in a quantitative manner. For the other two directions they have determined the damping constant α. First, we discuss shortly the last column of Table II. Clearly, our fitting procedure reveals a finite residual linewidth between 5 and 70 Oe depending on the orientation of the external field. As seen from Fig. 3, this should be taken with care. One would need experimental data at lower frequencies, e.g., at 4 GHz and below for an unambiguous result. In analogy to the experimental results shown in the inset of Fig. 4 one may expect that experiments at very low frequencies might give a very narrow linewidth. It follows from the slope of the linear fits for the [110] and [001] direction that only Gilbert damping is significant for these directions. The authors of Ref. 23 explain that the resonance line is broadened by a contribution from spin pumping,[25] which is the reason why the damping parameter G is significantly higher than the bulk value[24,26] of Fe $G=0.8\times10^8$ s^{-1}. To convert α into G we assume a bulklike saturation magnetization. The curvature in the data for the [100] direction shows nicely that in this direction the two-magnon scattering mechanism with a finite Γ parameter is effective and can be analyzed in a quantitative manner. For this direction we have performed two different fits shown in Fig. 5: (i) The dashed-dotted line is a fit through all five datapoints with G, Γ, and ΔH_0 as parameters, whereas (ii) the solid line is a fit omitting the datapoint at 73 GHz and keeping G fixed to the value determined from the slope of the dashed line. Nevertheless, fit (i) gives an unreasonable result. A least-squares fit would result in zero Gilbert damping. Even in a weighted fit (shown by the parameters in Table II) the Gilbert-damping parameter would be almost four times smaller than expected from the measurements along the [110] direction and the residual linewidth ΔH_0 would be rather large, too. Furthermore this means that this G value is much smaller than for bulk Fe. This would also contradict the above mentioned idea of spin pumping enhancement since the *unperturbed* Gilbert damping must be even smaller. Indeed, fit (ii) with $\gamma\Gamma=38\times10^8$ s^{-1} and $G=1.31\times10^8$ s^{-1} seems to be more realistic.

TABLE II. Fit parameters for the $Pd_{200}Fe_{30}/GaAs(001)$ sample from Ref. 23. The values given in italics correspond to the solid line fit in Fig. 5 omitting the datapoint at 73 GHz.

Orientation	γ (Oe)	$\gamma\Gamma$ (10^8 s^{-1})	G (10^8 s^{-1})	α (10^{-3})	ΔH_0 (Oe)
$\vec{H}\|[100]$	260	46	0.35	1.23	70
$\vec{H}\|[100]$	*215*	*38*	*(1.31)*	*4.6*	*55*
$\vec{H}\|[110]$	0	0	1.31	4.6	48
$\vec{H}\|[001]$	0	0	1.36	4.8	5

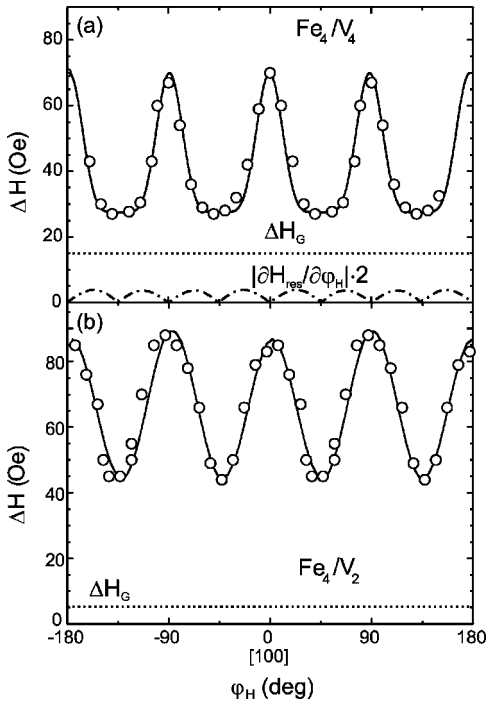

FIG. 6. Azimuthal angular dependence of the linewidth for (a) the Fe_4/V_4 and (b) the Fe_4/V_2 sample at 9 GHz. The dotted lines correspond to the Gilbert-damping contribution given in Table I. The dashed-dotted line represents the symmetry of a linewidth contribution due to inhomogeneity, e.g., mosaicity or field dragging. For solid lines, see text.

To corroborate our findings on two-magnon scattering, we present in Figs. 6 and 7 angle-dependent linewidth measurements for the Fe_4/V_4 and Fe_4/V_2 superlattice samples and compare the various linewidth contributions. φ_H and θ_H denote the angles of the external magnetic field measured with respect to the [100] and [001] axis, respectively. Figures 6(a) and 6(b) show the in-plane angle-dependent measurements for (a) the Fe_4/V_4 sample and (b) the Fe_4/V_2 sample. A clear fourfold symmetry is apparent. In contrast, the Gilbert damping [Eq. (3)] alone (dotted line) would not give rise to an in-plane angular dependence since for that G itself would have to be angle dependent. How can this be understood then? Neither mosaicity nor broadening by field dragging[10] lead to a fourfold symmetric line broadening, these have an

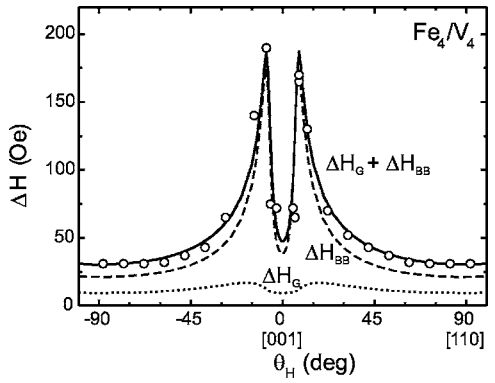

FIG. 7. Polar angular dependence for Fe_4/V_4 measured at 9 GHz. The solid line fit is the sum of the Gilbert-damping contribution (dotted line) and a T_2-Bloch-Bloembergen-type relaxation due to two-magnon scattering (dashed line). The damping parameters are the same as derived from the frequency dependence shown in Fig. 4.

eightfold symmetry (dashed-dotted line). On the other hand, as briefly discussed in Refs. 18 and 11, the rectangular surface defects cause the angle-dependent two-magnon scattering linewidth to vary like $\cos^2(2\varphi)$, where φ is the angle between $\vec{M}$ and the [100] axis.

As indicated by the solid lines in Figs. 6(a) and 6(b), this contribution is minimal in the [110] direction ($\varphi=45°$). In other words, the interface defects seem to be oriented mostly along the [100] direction, which is consistent with the findings from the frequency dependence shown in Table I, where Γ was larger for $\vec{H}\|[100]$ than for $\vec{H}\|[110]$. The Fe_4/V_4 sample [Fig. 6(a)] shows a slight deviation from this $\cos^2$ behavior. Here, we superimposed a $\cos^4(2\varphi)$ contribution to fit the angular dependence. That contribution might arise from a slightly different symmetry of the surface defects,[23] which also would account for the different two-magnon scattering strength of both samples. Also, the overall linewidth for this sample is different (smaller) than for the Fe_4/V_2 sample.

The corresponding polar angular dependence of the linewidth for the Fe_4/V_4 sample is shown in Fig. 7. Again, Gilbert damping alone (shown by the dotted line) is insufficient to reproduce the data, because the LLG is inadequate to describe a relaxation by two-magnon scattering.[5] The two-magnon scattering is ineffective close to the perpendicular orientation[11,12] and therefore a steep decrease is observed around $\theta_H \approx 0$. Nevertheless, this is completely different from the small decrease visible for ΔH_G that would result from the drag of the magnetization behind the external static field. Taking the transverse Bloch-Bloembergen-type (T_2) relaxation into account,[27]

$$\Delta H_{BB}(\theta_H) = \frac{dH_{res}}{d\omega_{res}} \frac{1}{T_2}, \tag{5}$$

where $dH_{res}/d\omega_{res}$ is easily calculated from the resonance equation, one can fit the data by a sum of Eqs. (3) and (5) with $1/T_2 \approx 7.1 \times 10^8$ s^{-1} as shown by the solid line in Fig. 7. This fit follows well the experimental data in Fig. 7 and thus enables one to separate the Gilbert damping from the two-magnon scattering contribution. Figures 6 and 7 also demonstrate that in these samples the Gilbert damping is clearly dominated by two-magnon scattering.

IV. CONCLUSIONS

Frequency dependent FMR measurements on various magnetic nanostructures show a clear nonlinear ω dependence of the linewidth $\Delta H(\omega)$. This is interpreted as resulting from a superposition of two relaxation processes: (i) the well-known Gilbert damping, i.e., a viscous, velocity proportional damping (like in Stokes friction) with energy dissipation to the thermal bath, and (ii) a scattering of spin wave excitations within the magnetic subsystem. Arias and Mills[11] have given a theoretical model in which the frequency dependence of the FMR linewidth is given by Eq. (4) for this kind of spin wave excitations. This relaxation channel (path No. 2 in Fig. 1) is determined independently in two experiments. The frequency dependence [Eq. (4)] yields $\approx 8 \times 10^8$ s^{-1} and the polar angular dependence $\approx 7 \times 10^8$ s^{-1}, in perfect agreement. Certainly, in the long run the spin wave excitation energy will also be transferred to the thermal bath. The two-magnon scattering is of particular importance in magnetic nanostructures and is less important in bulk ferromagnets, because real magnetic superlattices and ultrathin films have steps and defects on a length scale of some hundreds of nanometers. This is the order of magnitude for long-wavelength magnons of $k \approx 10^4$ cm^{-1} into which the uniform motion of magnetization can scatter.

Our present experiments performed over a very large range in frequency unambiguously confirm the presence and allow the separation of the two processes given by Eqs. (3) and (4), Gilbert damping and two-magnon scattering, respectively. Angle-dependent experiments and the use of Eq. (4) are in perfect agreement with this analysis. However, further work will be needed to bridge theory and experiment, i.e., the theory needs highly symmetric structures to calculate the scattering whereas real nanostructures have complex distributions and various kinds of defects. It will always be difficult to compare a hypothetical structural model needed as input for calculations with the real composition of interfaces of nanostructures.

The analysis and the results given in Tables I and II lead to a more satisfactory physical picture than the use of an "effective" Gilbert damping constant α_{eff} as an arbitrary fit parameter. The viscous Gilbert damping appears in our analyses as a constant characteristic of each particular material, like Fe, Co, Ni that is only slightly modified by spin pumping. On the other hand an evaluation of data assuming an effective Gilbert damping constant that changes by more than a factor of 10 for various samples of the same material and where the "constant" itself is frequency dependent (see Ref. 28) provides in our view very little insight to the understanding of scattering processes.

We suggest that the interpretation of the dynamics of the magnetization in nanostructures and interfaces should be performed in two steps. First, switching the direction of magnetization or, equivalently, a uniform motion of magnetization creates excitations in the magnetic subsystem (excited spin-waves with $k \neq 0$, transverse relaxation of magnon-magnon scattering). These excitations relax only later, in a second step, into the thermal bath.

ACKNOWLEDGMENTS

We thank P. Blomquist and R. Wäppling for providing the samples. Continuous discussions with J. Lindner and D. L. Mills are acknowledged. This work was supported by the DFG (Sfb290 TP A2) and Hungarian state Grants Nos. OTKA T043255 and TS049881.

*Author to whom correspondence should be addressed. Email address: babgroup@physik.fu-berlin.de

[1] L. Landau and E. Lifshitz, Phys. Z. Sowjetunion **8**, 153 (1935).
[2] T. L. Gilbert, Ph.D. dissertation, Illinois Institute of Technology, 1956.
[3] *Ultrathin Magnetic Structures II*, edited by B. Heinrich and J. A. C. Bland (Springer-Verlag, Berlin, 1994).
[4] *Ultrathin Magnetic Structures III*, edited by J. A. C. Bland and B. Heinrich (Springer-Verlag, Berlin, 2005).
[5] M. Sparks, *Ferromagnetic-Relaxation Theory* (McGraw-Hill, New York, 1964).
[6] *Magnetism*, edited by G. T. Rado and H. Suhl (Academic, New York, 1963), Vol. 1.
[7] H. Suhl, IEEE Trans. Magn. **34**, 1834 (1998).
[8] F. Bloch, Phys. Rev. **70**, 460 (1946); N. Bloembergen, *ibid.* **78**, 572 (1950).
[9] *Electron Paramagnetic Resonance of Transition Ions*, edited by A. Abragam and B. Bleaney (Clarendon, Oxford, 1970).
[10] Yu. V. Goryunov, N. N. Garif'yanov, G. G. Khaliullin, I. A. Garifullin, L. R. Tagirov, F. Schreiber, Th. Mühge, and H. Zabel, Phys. Rev. B **52**, 13450 (1995).
[11] R. Arias and D. L. Mills, Phys. Rev. B **60**, 7395 (1999).
[12] R. Arias and D. L. Mills, J. Appl. Phys. **87**, 5455 (2000).
[13] D. L. Mills and S. M. Rezende, Top. Appl. Phys. **87**, 27 (2003).
[14] Equation (4) follows from Eq. (100) of Ref. 11 if one transforms the field dependence into a frequency dependence. The authors of Ref. 11 suggest that this approximation should be used when fitting real experiments. The full theoretical expression is given in Eq. (94) of Ref. 11. There, a regular geometric structure for easier calculation of matrix elements is assumed. The two results differ only by a few percent.
[15] Z. Celinsky and B. Heinrich, J. Appl. Phys. **70**, 5935 (1991).
[16] T. Fehér, A. Jánossy, G. Oszlányi, F. Simon, B. Dabrowski, P. W. Klamut, M. Horvatić, and G. V. M. Williams, Phys. Rev. Lett. **85**, 5627 (2000).
[17] See the European high field-EPR network, http://www.sentinel2004.org/
[18] J. Lindner, K. Lenz, E. Kosubek, K. Baberschke, D. Spoddig, R. Meckenstock, J. Pelzl, Z. Frait, and D. L. Mills, Phys. Rev. B **68**, 060102(R) (2003); J. Magn. Magn. Mater. **272–276**, e1653 (2004). Note that for the numbers given in this reference a different fitting procedure was used and a factor in Eqs. (3) and (4) was missing.
[19] P. Isberg, B. Hjörvarsson, R. Wäppling, E. B. Svedberg, and L. Hultman, Vacuum **48**, 483 (1997).
[20] A. N. Anisimov, W. Platow, P. Poulopoulos, W. Wisny, M. Farle, K. Baberschke, P. Isberg, B. Hjörvarsson, and R. Wäppling, J. Phys.: Condens. Matter **9**, 10581 (1997).
[21] A. N. Anisimov, M. Farle, P. Poulopoulos, W. Platow, K. Baberschke, P. Isberg, R. Wäppling, A. M. N. Niklasson, and O. Eriksson, Phys. Rev. Lett. **82**, 2390 (1999).
[22] Measurements were done at the Freie Universität Berlin, at the Academy of Sciences of the Czech Republic, and at the Budapest University of Technology and Economics.
[23] G. Woltersdorf and B. Heinrich, Phys. Rev. B **69**, 184417 (2004).
[24] M. B. Stearns, in *Magnetic Properties of Metals*, Landolt-Börnstein, New Series, edited by H. P. J. Wijn (Springer, Berlin, 1986), Vol. III/19a.
[25] Y. Tserkovnyak, A. Brataas, and G. E. W. Bauer, Phys. Rev. Lett. **88**, 117601 (2002).
[26] S. T. Purcell, B. Heinrich, and A. S. Arrott, J. Appl. Phys. **64**, 5337 (1988).
[27] M. J. Hurben, D. R. Franklin, and C. E. Patton, J. Appl. Phys. **81**, 7458 (1997).
[28] G. Woltersdorf, M. Buess, B. Heinrich, and C. H. Back, Phys. Rev. Lett. **95**, 037401 (2005).